Mono- or Diphenylpyridazines Connected to *N*-(2,4-Difluorophenyl)-*N*′-heptylurea as Acyl-CoA:Cholesterol Acyltransferase Inhibitors

Arianna Gelain,[†] Ilaria Bettinelli,[†] Daniela Barlocco,*[,†] Byoung-Mog Kwon,[‡] Tae-Sook Jeong,[‡] Kyung-Hyun Cho,[‡] and Lucio Toma*[,§]

Istituto di Chimica Farmaceutica e Tossicologica, Università di Milano, Viale Abruzzi 42, 20131 Milano, Italy, Korea Research Institute of Bioscience & Biotechnology, 52 Uen-Dong Yusung-Ku, Taejeon 305-600, South Korea, and Dipartimento di Chimica Organica, Università di Pavia, Via Taramelli 10, 27100 Pavia, Italy

Received July 22, 2005

Mono- and diphenylpyridazine ureido derivatives, structurally related to DuP 128, were synthesized and tested for their inhibitory activity against ACAT isolated from rat liver microsomes. Several compounds displayed ACAT inhibition in the micromolar range. The amino derivatives **4a**−**c** were also tested against hACAT-1 and hACAT-2 isoforms. They retained the same trend shown in the previous assay. Modeling studies on representative terms were performed. Significant similarities between the geometrical features of the model DuP 128 and the most active pyridazine derivatives were observed.

Introduction

Atherosclerosis and related cardiovascular diseases, such as coronary heart disease (CHD), represent the major cause of death in the industrialized countries.[1] Although statin drugs are powerful weapons against atherosclerosis, CHD risk remains high, making it desirable to develop additional therapeutic approaches,[2] including the inhibition of acyl-CoA:cholesterol acyltransferase (ACAT). This enzyme catalyzes cholesterol esterification and plays an important role in lipoprotein assembly, dietary cholesterol absorption, and intracellular cholesterol metabolism.[3] Most relevant to CHD is that in the arterial wall, cholesteryl esters produced by the form of ACAT known as ACAT-1 can accumulate in macrophages and smooth muscle cells to produce foam cells, leading to plaque initiation and atherosclerotic progression.[4−6] On the other hand, the selective distribution of ACAT-2 in the endoplasmatic reticulum of liver and intestine seems to suggest that this isoenzyme could operate in a specialized manner, for example in intestinal cholesterol absorption and in lipoprotein secretion.[6,7] On the basis of this evidence, it has been proposed that ACAT inhibitors could be useful in the treatment of atherosclerosis and related disorders.

In previous papers, some of us reported a series of alkyl-5,6-diphenylpyridazine derivatives showing a micromolar range inhibition toward ACAT. These compounds retained several main features of ACAT inhibitors, such as a long alkyl side chain linked to a heterocycle by a heteroatom of different nature and the *o*-diphenyl system.[8] To better define the structural requirements of this class, a series of derivatives with different substituents both on the *o*-diphenyl system and the side-chain were also synthesized.[9−11]

Chart 1

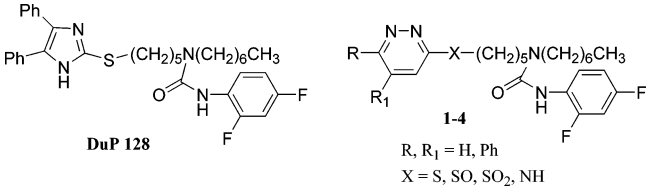

As a part of our ongoing research program, we describe herein the design, the synthetic approach, the results of the enzyme assay, and the conformational study for novel series of compounds (**1**−**4**), structurally related to DuP 128, a potent ureido derivative, which antagonizes ACAT from rat hepatic microsomes with an IC_{50} = 10 nM (Chart 1).[12] Compounds **1**−**4** combine the characteristic substituted urea of DuP 128 with pyridazine, which serves as the central ring template. Moreover, the role of the two phenyl groups attached to the heterocycle was evaluated by studying the analogues depleted of the phenyl group at the 5 or 6 position of pyridazine, respectively.

Chemistry

The thio derivatives (**1a**−**c**) were obtained following the method reported in the literature for the analogous imidazole derivatives.[12] Accordingly, δ-valerolactone was reacted with *n*-heptylamine in boiling toluene to give the amide (**5**) which was reduced to the corresponding amine (**6**) by lithium aluminum hydride. Condensation of **6** with difluorophenyl isocyanate in dichloromethane gave the ureido derivative **7**, which was treated with tetrabromomethane to give **8**, eventually condensed with the required pyridazinethiol (**9a**−**c**), in turn obtained from the corresponding pyridazinones[8,13,14] by treatment with Lawesson's reagent. Subsequent oxidation with oxone gave a mixture of the corresponding sulfoxides (**2a**−**c**) and sulfones (**3a**−**c**), which were easily separated by flash chromatography (Scheme 1, Table 1).

* Corresponding authors: (D.B.) Tel +39.02.50317515 Fax +39.02.50317565 E-mail: daniela.barlocco@unimi.it. (L.T.) Tel. +39.0382. 987843 Fax +39.0382.987323 E-mail: lucio.toma@unipv.it.
† Istituto di Chimica Farmaceutica e Tossicologica.
‡ Korea Research Institute.
§ Dipartimento di Chimica Organica.

10.1021/jm050703x CCC: $30.25
Published on Web 11/05/2005

Scheme 1

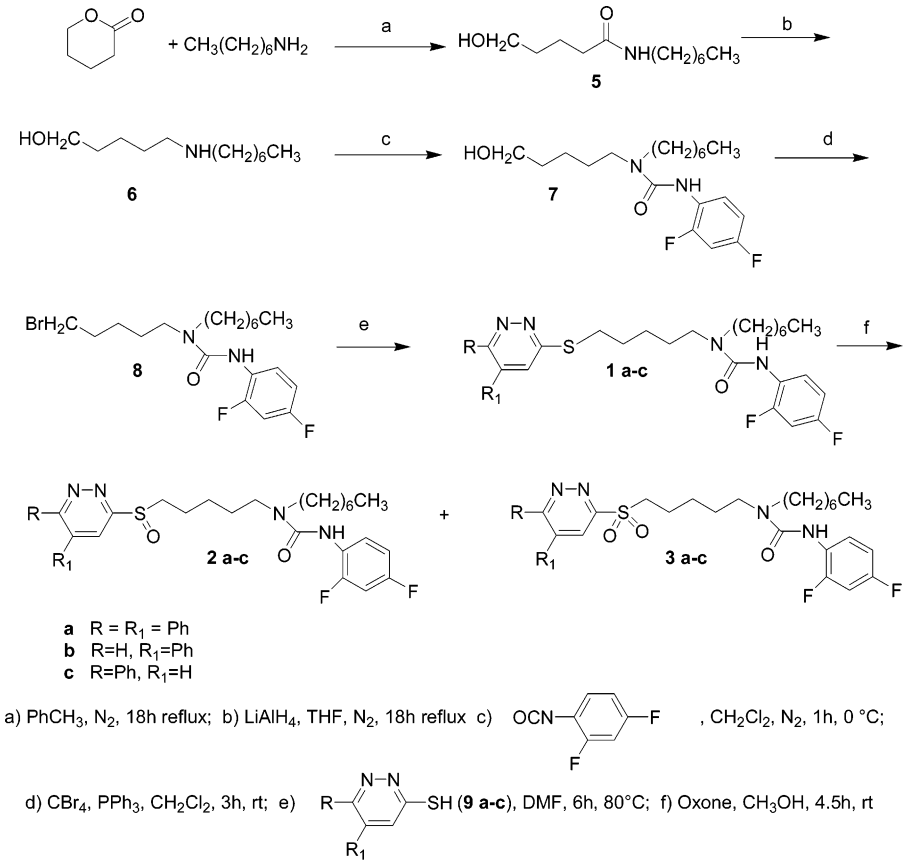

Table 1. Chemical Data and Rat ACAT Inhibition of Pyridazine Derivatives and GERI-BP001M

compd	R	R_1	X	% yield	formula[a]	% inhibition[b] at 50 μg/mL
1a	Ph	Ph	S	55[c]	$C_{35}H_{40}F_2N_4OS$	75
1b	H	Ph	S	46[c]	$C_{29}H_{36}F_2N_4OS$	75
1c	Ph	H	S	79[c]	$C_{29}H_{36}F_2N_4OS$	44
2a	Ph	Ph	SO	29[d]	$C_{35}H_{40}F_2N_4O_2S$	65
2b	H	Ph	SO	6[d]	$C_{29}H_{36}F_2N_4O_2S$	62
2c	Ph	H	SO	8[d]	$C_{29}H_{36}F_2N_4O_2S$	55
3a	Ph	Ph	SO_2	12[d]	$C_{35}H_{40}F_2N_4O_3S$	70
3b	H	Ph	SO_2	17[d]	$C_{29}H_{36}F_2N_4O_3S$	67
3c	Ph	H	SO_2	73[d]	$C_{29}H_{36}F_2N_4O_3S$	43
4a	Ph	Ph	NH	66[e]	$C_{35}H_{41}F_2N_5O$	87
4b	H	Ph	NH	63[e]	$C_{29}H_{37}F_2N_5O$	46
4c	Ph	H	NH	55[e]	$C_{29}H_{37}F_2N_5O$	89
GERI-BP001M						83

[a] C, H, N analysis within ±0.4%. [b] In vitro % ACAT inhibition determined in rat liver microsomes. All values are means from three experiments, which differ by less than 10%. [c] From **8**. [d] From **1a**−**c**. [e] From **13a**−**c**.

The synthesis of the amino derivatives (**4a**−**c**) was depicted in Scheme 2. The required chloropyridazine (**10a**−**c**) was condensed with 1,5-pentanediamine to give the corresponding **11a**−**c**, which was reacted with *n*-heptanoyl chloride. The so obtained amides (**12a**−**c**) were reduced by lithium aluminum hydride to **13a**−**c** and finally treated with difluorophenyl isocyanate in dichloromethane to give the desired **4a**−**c**.

Pharmacological Results

All compounds were tested for their inhibitory properties toward ACAT extracted from rat liver microsomes. Their activity, expressed as inhibition percentage at 50 μg/mL, is shown in Table 1. Among the thio derivatives, **1a** and **1b** showed the best activity with an inhibition percentage of 75. By contrast, the 6-phenyl derivative (**1c**) was a very weak inhibitor (44%). It should be noted that oxidation of **1a**,**b** to their corresponding sulfoxides (**2a**,**b**) and sulfones (**3a**,**b**) led to a significant loss of potency, though by different degrees.

Among the amino derivatives, the most interesting activity was found in compounds **4a** and **4c** (87% and 89% inhibition, respectively), while the 5-phenyl derivative (**4b**) had a much lower potency (46% inhibition). The inhibitory properties of the amino series **4a**−**c**, to which the two best compounds belong, were also checked on the human ACAT-1 and ACAT-2 isoforms. A trend similar to that seen in microsomial ACAT was found (Table 2). No significant selectivity between the two isoforms was shown by the active compounds **4a**,**c** as already seen in the case of DuP 128.[15]

Modeling

A modeling study of compounds **1a**−**4a**, in comparison with DuP 128, was performed in order to attempt a rationalization of the activity of the different series of compounds on geometrical grounds. Thus, simplified model structures, **14**−**18** (Chart 2), were chosen for the theoretical calculations where the invariant substituted ureido group was shortened to a *n*-butyl chain. The energy profiles for rotation around the C3−X bond were initially determined on the models unsubstituted at the 5 and 6 positions of the heterocyclic ring. Then, after

Scheme 2

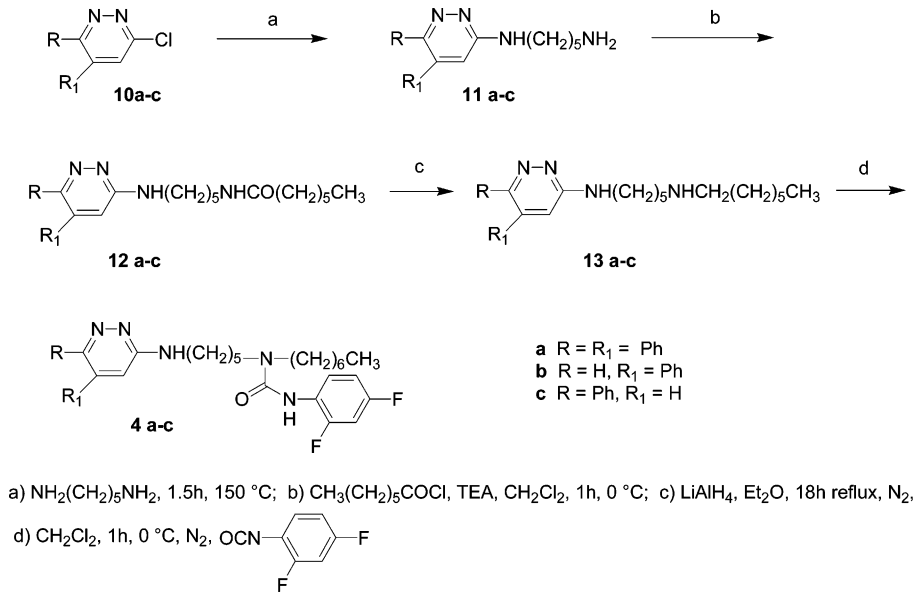

Table 2. Rat and Human ACAT Inhibition of Compounds **4a**−**c**

compd	rat ACAT,[a] IC_{50} (μM)[c]	hACAT-1,[b] IC_{50} (μM)[c]	hACAT-2,[b] IC_{50} (μM)[c]
4a	2.32	0.94	1.74
4b	36.4	414	101
4c	1.21	5.34	2.07

[a] See ref 16. [b] See refs 17, 18. [c] All values are means from three experiments which differ by less than 10%.

Chart 2

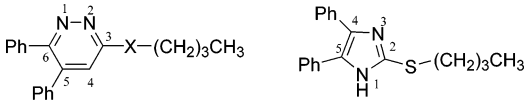

Table 3. Relative Energy and Selected Geometrical Data of the Preferred Conformations of Compounds **14**−**18**

conformation	E_{rel} (kcal/mol)	$\tau 1$[a] (deg)	$\tau 2$[b] (deg)
14A	0.00	1	−179
14B	2.91	−179	178
15A	0.00	65	180
15B	5.29	−41	171
16A	0.00	44	−175
17A	0.00	−166	176
17B	0.13	11	−174
18A	0.00	10	−177

[a] Torsional angle defined by N3−C2−S−CH_2 for **18** and by N2−C3−X−CH_2 for **14**−**17**. [b] Torsional angle defined by C2−S−CH_2−CH_2 for **18** and by C3−X−CH_2−CH_2 for **14**−**17**.

addition of the 5- and 6-phenyl groups to the minima located in the profiles, the structures were optimized, allowing determination of the minimum energy conformations of compounds **14**−**18** reported in Table 3. Two minima were located for **14**, **15**, and **17** whereas only one minimum was located for **16** and **18**. In the case of sulfide **14** and sulfoxide **15** the difference in energy between the two conformers is large enough to ensure that only one conformer is significantly populated while, in the case of amine **17**, the two conformers are almost isoenergetic and hence almost equally populated. The populated conformations of each compound are reported in Figure 1. In the hypothesis that the ureido function of all the compounds interacts in the same way at the binding site inducing a similar orientation of the alkyl chain, we performed a comparison of the geometry of the populated conformations of **14**−**17** with **18A** by superimposing the butyl chain and evaluating the differences in the orientation of the diphenylheterocyclic moiety (Figure 2). The distances between the centroids of the phenyl groups (d_C) of each couple of molecules in comparison were measured and are reported in Figure 2. The two conformers of the amino derivative **17** are compared with **18A** in Figures 2A,B, respectively. It can easily be seen that only **17A** compares well with **18A** while conformer **17B** orients its phenyl groups in different regions; this suggests that **17A** might represent the active conformation of the amino derivative **4a**. Moreover, the 6-phenyl group of **17A** matches quite well the 5-phenyl group of **18A** (d_C = 0.49 Å) while the 5-phenyl group matches the 4-phenyl group (d_C = 1.08 Å). Also the thioether derivative **14A** gives an acceptable overlap with **18A** though one phenyl group slightly deviates (Figure 2 C); however, it is worth noting that, in this case, the 5-phenyl group of **18A** is matched by the 5-phenyl group of **14A** (d_C = 0.88 Å). In addition, it should be observed that **17A**, **14A**, **18A** present almost planar geometries; in fact, the torsional angle $\tau 1$ (defined in Table 3) is very close to 180° (**17A**) or to 0° (**14A** and **18A**) whereas the torsional angle $\tau 2$ is always very close to 180°. By contrast, **15A** and **16A**, show a significant deviation from planarity ($\tau 1$ = 65° and 44°, respectively) and very poor superimpositions in the comparison with **18A** (Figure 2D,E).

Discussion

The pharmacological results are quite intriguing as the most active compounds appear randomly scattered among the different series of compounds. In particular, the 5,6-diphenyl derivatives **1a** and **4a** are appreciably active as well as the 5-phenyl analogue **1b** and the 6-phenyl analogue **4c**, belonging to the thioether and to the amino series, respectively. All compounds in the

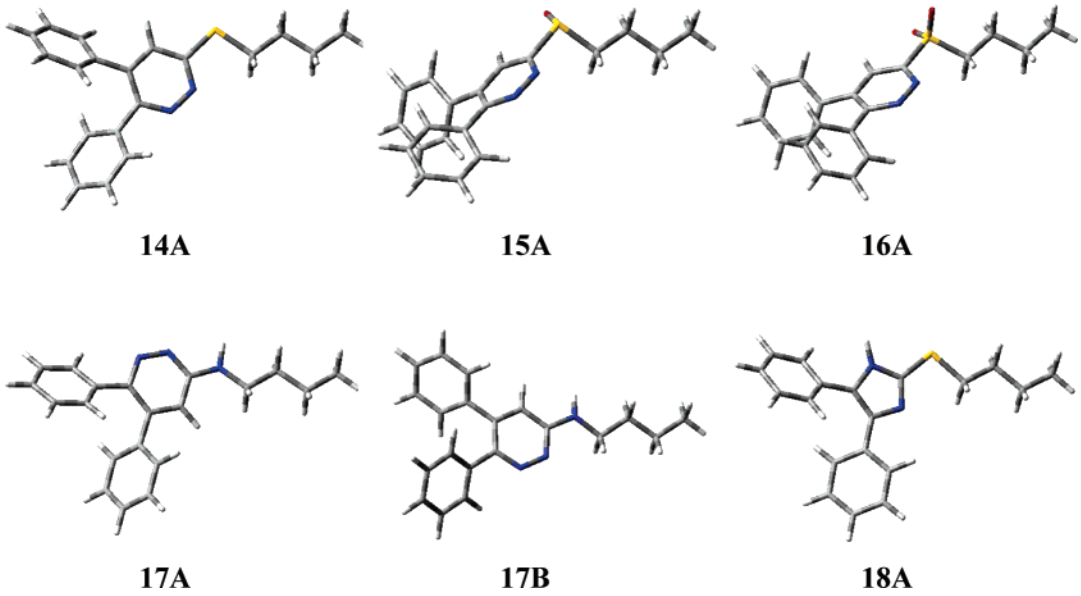

Figure 1. Three-dimensional plots of the preferred conformations of compounds **14**−**18**.

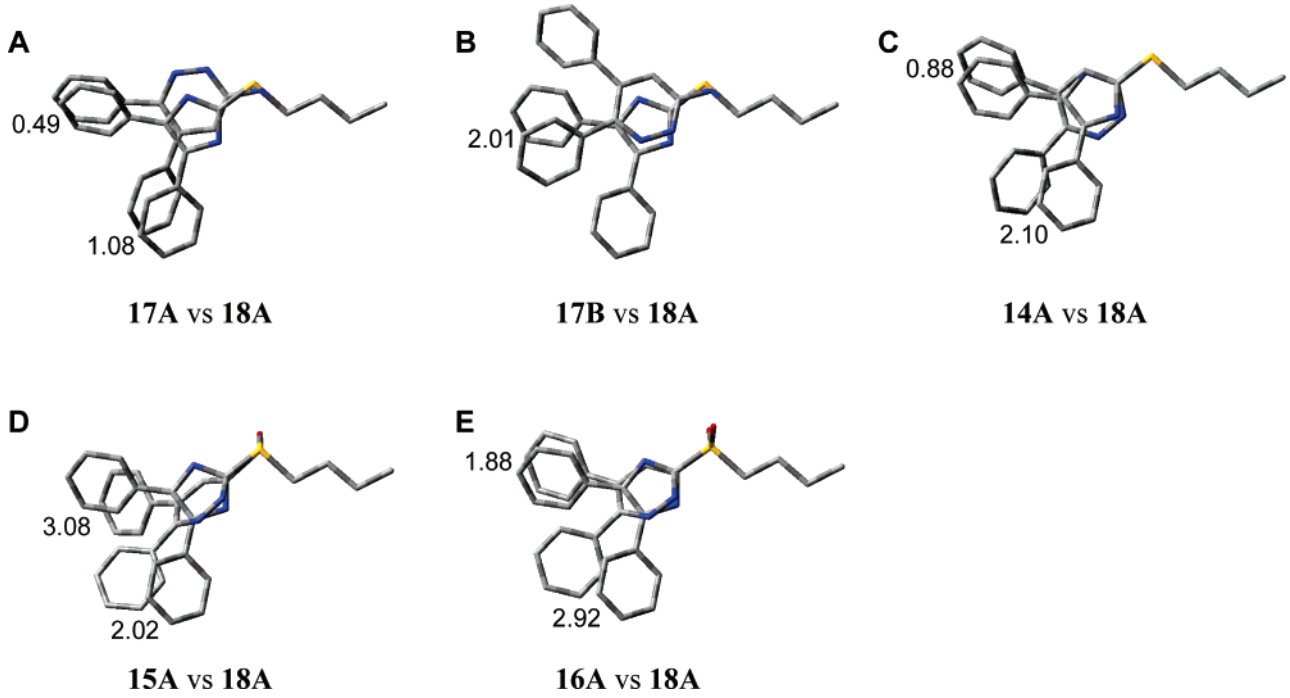

Figure 2. Superimposition of conformation **18A** with the preferred conformations of compounds **14**−**17**.

sulfoxide **2** and to the sulfone **3** series are appreciably less active. The different behavior might rely on several reasons (e.g. the different nature of the X functional groups, the electronic or electrostatic properties, the ability to function as hydrogen bond donors or acceptors). However, if the X group simply acts as linker between the pyridazine and the alkyl chain, its effect might be due to geometrical constraints that can modify the overall shape of the molecules.

The pharmacological results, combined with the modeling studies, suggest that the geometrical factors could prevail. In fact, two items, focused by the modeling, fairly correlates with activity. The first one is the planarity at the junction of the alkyl chain with pyridazine, as compounds that greatly deviate from planarity are less active (sulfoxide and sulfone series). The second item is connected to the role of the two phenyl groups. Inhibition data show that only one phenyl group is required for activity, namely the 6-phenyl (**4c**) in the amino series and the 5-phenyl (**1b**) in the thioether series; the other phenyl group might probably be unnecessary, though it does not create any steric interaction. The apparent contradiction that in one case the phenyl is present in 5, while in the other it is in 6, is easily solved by the models. In fact, Figure 3 shows that compounds **1b** and **4c** in their active conformations orient the pyridazine ring in opposite ways, due to the different torsional angle at the C3−X bond (τ1 about 180° in the amino series and about 0° in the thioether series), Therefore, the binding of their phenyl group to the same pocket of the receptor is allowed. Finally, compounds of the **2** and **3** series, being nonplanar, cannot correctly orient any of their phenyl groups.

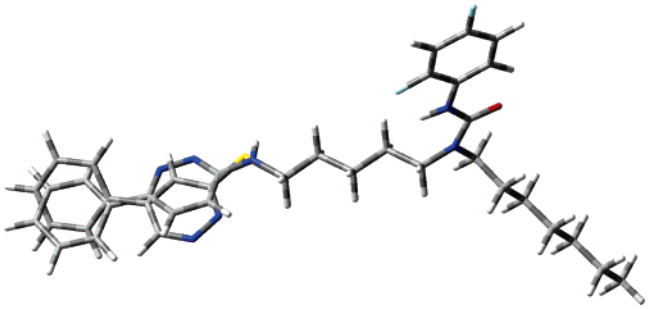

Figure 3. Superimposition of compounds **1b** and **4c**.

Experimental Section

Chemistry. Melting points were determined on a Büchi 510 capillary melting points apparatus and are uncorrected. ^{1}H NMR spectra were recorded on a Bruker AC200 spectrometer; chemical shifts are reported as δ (ppm), using the solvent as internal standard. Merck F-254 commercial plates were used for analytical TLC to follow the course of reaction and check product purity. Silica gel 60 (Merck, 230−400 mesh) was used for flash chromatography. Elemental analyses of all new compounds were within ±0.4 of the theoretical values. The structures of all compounds were consistent with their analytical and spectroscopic data.

General Procedure for the Synthesis of the Thio Derivatives 1a−c, 2a−c, 3a−c. (a) A solution of δ-valerolactone (5.0 g, 50 mmol) and *n*-heptylamine (9 mL, 60 mmol) in toluene (10 mL) was refluxed for 18 h in a nitrogen atmosphere. After cooling, ethyl acetate (60 mL) was added to the mixture, which was washed in sequence with 1 N HCl (3 × 10 mL) and water (3 × 10 mL). After drying over sodium sulfate and evaporation of the solvent, *N*-heptyl-5-hydroxypentanamide **5** was obtained as a white solid (9.04 g, 84%), mp = 54−55 °C.[12]

(b) To a mixture of $LiAlH_4$ (0.26 g, 7 mmol) in anhydrous THF (12 mL) under nitrogen was added a solution of **5** (0.75 g, 3.5 mmol) in anhydrous THF (4 mL) dropwise. The mixture was then refluxed for 18 h. After cooling to 0 °C, a 10% aqueous solution of Na_2SO_4 (3 mL) was added, the solid filtered off, and the mixture extracted with ethyl acetate (3 × 10 mL). The organic layer was washed with aqueous NaCl (3 × 5 mL), dried over sodium sulfate, and evaporated under vacuum to give *N*-heptyl-5-hydroxypentanamine **6**[12] (0.54 g, 77%).

(c) To a solution of **6** (0.2 g, 0.99 mmol) in CH_2Cl_2 (1.28 mL) cooled to 0 °C was slowly added 2,4-difluorophenyl isocyanate (0.12 mL, 0.99 mmol) under nitrogen. The mixture was stirred for 1 h and then poured into 1 N HCl (5 mL) and extracted with ethyl acetate (3 × 10 mL). The organic layer was washed in sequence with water and an aqueous solution of NaCl (3 × 5 mL). After drying over sodium sulfate and evaporation of the solvent, the oily yellow residue was purified by flash chromatography (eluent CH_2Cl_2/CH_3OH 98/2) to give *N*-(2,4-difluorophenyl)-*N*′-heptyl-*N*′-(5-hydroxypentyl)urea **7**[12] (0.050 g, 50%).

(d) To a solution of **7** (0.075 g, 0.21 mmol) and CBr_4 (0.083 g, 0.25 mmol) in CH_2Cl_2 (2 mL) under nitrogen was added slowly a solution of PPh_3 (0.067 g, 0.25 mmol) in CH_2Cl_2 (0.5 mL), and the mixture was stirred for 3 h at room temperature. The so obtained oily mixture was purified by flash chromatography (eluent petroleum ether/EtOAc 9/1) to give *N*-(2,4-difluorophenyl)-*N*′-heptyl-*N*′-(5-bromopentyl)urea **8**[12] (0.060 g, 68%).

(e) A mixture of the appropriate pyridazinethiol (**9a−c**, 0.12 mmol), anhydrous K_2CO_3 (0.065 mg, 0.48 mmol), and **8** (0.10 g, 0.24 mmol) in anhydrous DMF (0.5 mL) was stirred at 80 °C for 6 h. To the cooled solution, water was added (2 mL), and the mixture was extracted with CH_2Cl_2 (3 × 10 mL). After drying, the solvent was evaporated under vacuum to give the final compounds (**1a−c**), which were purified by flash chromatography (eluent cyclohexane/EtOAc 75/25).

N-(2,4-Difluorophenyl)-*N*′-heptyl-*N*′-{5-[(5,6-diphenylpyridazin-3-yl)thio]pentyl}urea **1a**: ^{1}H NMR ($CDCl_3$) δ: 0.85 (t, 3H); 1.20−1.35 (m, 8H); 1.50−1.75 (m, 6H); 1.85−1.95 (m, 2H); 3.25−3.35 (m, 4H); 3.40−3.45 (t, 2H); 6.40−6.45 (br s, 1H); 6.75−6.85 (m, 2H); 7.15−7.20 (m, 2H); 7.25−7.40 (m, 9H); 8.00−8.05 (m, 1H).

(f) To a solution of the appropriate **1a−c** (0.094 mmol) in methanol (2.5 mL) was added oxone (0.119 g, 0.19 mmol) portionwise and the mixture stirred for 4.0 h. The residue was treated with methanol (10 mL) and filtered. After evaporation of the solvent, the mixture of **2** and **3** was purified by flash chromatography (eluent cyclohexane/EtOAc 60/40) (See Table 1 and Supporting Information).

N-(2,4-Difluorophenyl)-*N*′-heptyl-*N*′-{5-[(5,6-diphenylpyridazin-3-yl)sulfinyl]pentyl}urea **2a**: ^{1}H NMR ($CDCl_3$) δ: 0.85 (t, 3H); 1.20−2.00 (m, 16H); 3.25−3.60 (m, 6H); 6.40−6.45 (br s, 1H); 6.75−6.85 (m, 2H); 7.30−7.55 (m, 9H); 7.70−7.75 (m, 1H); 8.00−8.05 (m, 1H); 8.15 (s, 1H).

N-(2,4-Difluorophenyl)-*N*′-heptyl-*N*′-{5-[(5,6-diphenylpyridazin-3-yl)sulfonyl]pentyl}urea **3a**: ^{1}H NMR ($CDCl_3$) δ: 0.85 (t, 3H); 1.20−1.40 (m, 8H); 1.50−1.70 (m, 6H); 1.95−2.00 (m, 2H); 3.25−3.35 (m, 4H); 3.70−3.75 (t, 2H); 6.40 (br s, 1H); 6.80−6.85 (m, 2H); 7.20−7.50 (m, 10H); 8.00−8.05 (m, 1H); 8.15 (s, 1H).

General Procedure for the Synthesis of the Amino Derivatives 4a−c. To the appropriate chloropyridazine (**10a−c**, 0.3 mmol) was added 1,5-pentanediamine (3 mmol), and the mixture was stirred at 150 °C for 1.5 h. The so obtained **11a−c** were purified by flash chromatography (eluent CH_2Cl_2/$CH_3OH.NH_3$ 98/2).

[5-(5,6-Diphenylpyridazin-3-yl)amino]pentanamine **11a** (Y = 88%): ^{1}H NMR ($CDCl_3$) δ: 1.40−1.55 (m, 4H); 1.65−1.80 (m, 2H); 2.15 (br s, 2H, exch with D_2O); 2.70 (t, 2H); 3.40−3.50 (m, 2H); 4.95 (br s, 1H, exch with D_2O); 6.60 (s, 1H); 7.10−7.35 (m, 10H).

To a solution of the appropriate diamine **11a−c** (2.05 mmol) and TEA (2.24 mmol, 0.31 mL) in dichloromethane (5 mL) cooled at 0 °C under nitrogen was added *n*-heptanoyl chloride (2.05 mmol, 0.32 mL) dropwise. After 1 h stirring, the mixture was poured into water and extracted with dicloromethane (3 × 10 mL). The organic layer was washed with brine, dried over magnesium sulfate, and evaporated under vacuum. The residue was purified by flash chromatography (eluent $CHCl_2$/CH_3OH 95/5) to give the amides **12a−c**.

N-{[5-(5,6-Diphenylpyridazin-3-yl)amino]pentyl}heptanamide **12a** (Y = 44%): ^{1}H NMR ($CDCl_3$) δ: 0.85 (t, 3H); 1.20−1.30 (m, 6H); 1.40−1.60 (m, 6H); 1.65−1.75 (m, 2H); 2.10−2.15 (t, 2H); 3.20−3.25 (m, 2H); 3.45−3.50 (m, 2H); 5.35 (m, 1H); 5.95 (m, 1H); 6.65 (s, 1H); 7.10−7.35 (m, 10H).

To the appropriate amide **12a−c** (0.7 mmol) in anhydrous diethyl ether (0.5 mL) stirred under nitrogen was added $LiAlH_4$ (1.4 mmol, 0.053 g), and the mixture was refluxed for 18 h. After cooling to room temperature, the mixture was poured onto ice/water, the precipitate filtered off, and the solution extracted with ethyl acetate (3 × 10 mL). The organic layer was washed with brine, dried over magnesium sulfate, and evaporated under vacuum. The residue was purified by flash chromatography (eluent CH_2Cl_2/$CH_3OH.NH_3$ 95/5) to give the diamines **13a−c**.

N-{[(5,6-Diphenylpyridazin-3-yl)amino]pentyl}heptanamine **13a** (Y = 53%): ^{1}H NMR ($CDCl_3$) δ: 0.85 (t, 3H); 1.25−1.35 (m, 8H); 1.45−1.60 (m, 6H); 1.65−1.80 (m, 2H); 2.15 (m, 1H); 2.55−2.65 (m, 4H); 3.45−3.55 (m, 2H); 5.00 (m, 1H); 6.60 (s, 1H); 7.10−7.35 (m, 10H).

To the appropriate diamine (**13a−c**, 0.232 mmol) in anhydrous dichloromethane (1.5 mL) cooled at 0 °C under nitrogen was added slowly 2,4-difluorophenyl isocyanate (0.029 mL, 0.253 mmol), and the mixture stirred for 1 h, poured into 1 N HCl (1.7 mL), and extracted with ethyl acetate (3 × 10 mL). The organic layer was washed with brine, dried over magnesium sulfate, and evaporated under vacuum. The residue was purified by flash chromatography (eluent $CHCl_2$/CH_3OH 95/5) to give the desired compounds **4a−c**. (See Table 1 and Supporting Information).

N-(2,4-difluorophenyl)-*N*′-heptyl-*N*′-{5-[(5,6-diphenylpyridazin-3-yl)amino]pentyl}urea **4a**: ^{1}H NMR ($CDCl_3$) δ: 0.85 (t, 3H);

1.25−1.35 (m, 8H); 1.45−1.55 (m, 2H); 1.60−1.65 (m, 2H); 1.70−1.80 (m, 2H); 1.80−1.85 (m, 2H); 3.25−3.40 (m, 4H); 4.10−4.15 (m, 2H); 6.50 (br s, 1H); 6.80−6.95 (m, 4H); 7.20−7.45 (m, 8H); 7.95−8.05 (m, 2H); 12.60 (s, 1H).

General Procedure for the Synthesis of the Pyridazinethiols 9a−c. To a solution of the appropriate pyridazinone[8,13,14] (2 mmol) in toluene (120 mL) was added Lawesson's reagent (0.5 g, 12.4 mmol), and the solution was stirred at 130 °C for 3 h. After cooling, the solvent was evaporated under vacuum and the product purified by flash chromatography (eluent petroleum ether/EtOAc 8/2).

3-Mercapto-5,6-diphenylpyridazine **9a** (Y = 60%), ^{1}H NMR ($CDCl_3$) δ: 7.10−7.40 (m, 10H); 7.80 (s, 1H); 12.40 (br s, 1H).

General Procedure for the Synthesis of the Chloropyridazines 10a−c. A mixture of the appropriate pyridazinone[8,13,14] (0.65 mmol) and $POCl_3$ (1.5 mL, 16 mmol) was stirred at 60 °C for 3 h. After cooling, the mixture was poured onto ice/water (10 mL), its pH was brought to 6 by 5 N NaOH, and then it was extracted with CH_2Cl_2 (3 × 15 mL). After drying over sodium sulfate, evaporation of the solvent gave **10a−c**, which was used as such for the next step.

3-Chloro-5,6-diphenylpyridazine **10a** (Y = 70%): ^{1}H NMR ($CDCl_3$) δ: 7.15 (d, 2H); 7.30−7.40 (m, 8H); 7.55 (s, 1H).

Enzyme Assays. *In Vitro Assay against Rat ACAT.* Microsomes prepared from rat liver were used as a source of the enzyme. The activity of the ACAT inhibitors against rat ACAT was measured according to a previously described method.[16] GERI-BP001 M[16] was used as reference compound.

In vitro assay against hACAT-1 and hACAT-2. Microsomal fractions of Hi5 cells containing baculovirally expressed ACAT-1 or -2 were used as the sources of enzymes.[17] The activity of the hACAT-1 and hACAT-2 was measured according to the method of Brecher and Chan[18] with slight modification.[17]

Modeling. *Computational Methods*. All calculations were carried out using the Gaussian 03[19] program package. The conformational space of compounds **14−18** was explored through optimizations at the B3LYP level with the 6-31G* basis set. The energy profiles for rotation around the C3-X bond were initially determined on simplified molecules unsubstituted at the 5 and 6 positions of the heterocyclic ring. Then, after addition of the 5- and 6-phenyl groups to the minima located in the profiles, the structures were fully optimized allowing to determine the minimum energy conformations of compounds **14−18**.

Acknowledgment. This work was partially supported by Italy-Korea Joint Research Program and KRIBB Initiative Research Program. The authors also aknowledge the financial support from the University of Milan (FIRST 2004) and Pavia (FAR 2004).

Supporting Information Available: Physical properties and ^{1}H NMR data of compounds. This material is available free of charge via the Internet at http://pubs.acs.org.

References

(1) American Heart Associaton. *1999 Heart and Stroke Statistical Update*; American Heart Association: Dallas, TX, 1998.
(2) Norata, G. D.; Catapano, A. L. Lipid lowering activity of drugs affecting cholesterol absorption. *Nutr. Metab. Cardiovas. Dis.* **2004**, *14*, 42−51.
(3) Kushwaha, R. S.; Vandeberg, J. F.; Rodriguez, R.; Vandeberg, J. L. Cholesterol absorption and hepatic acyl-coenzyme A:cholesterol acyltransferase activity play major roles in lipemic response to dietary cholesterol and fat in laboratory opossums. *Metabolism* **2004**, *53*, 817−822.
(4) Chang, C. C. Y.; Lee, C. G..; Chang, E. T.; Cruz, J. C.; Levesque, M. C.; Chang, T. Y. Recombinant acyl-CoA: cholesterol acyltransferase-1 (ACAT-1) purified to essential homogeneity utilizes cholesterol in mixed micelles or in vesicles in a highly cooperative manner. *J. Biol. Chem.* **1998**, *273*, 35132−35141.
(5) Joyce, C.; Skinner, K.; Anderson, R. A.; Rudel, L. L. Acyl-coenzyme A: cholesteryl acyltransferase 2. *Curr. Opin. Lipidol.* **1999**, *10*, 89−95.
(6) Rudel, L. L.; Lee, R. G.; Cockman, T. L. Acyl coenzyme A: cholesterol acyltransferase types 1 and 2: structure and function in atherosclerosis. *Curr. Opin. Lipidol*. **2001**, *12*, 121−127.
(7) Song, B. L.; Qi, W.; Yang, X. Y.; Chang, C. C.; Zhu, J. Q.; Chang, T. Y.; Li, B. L. Organization of human ACAT-2 gene and its cell-type-specific promoter activity. *Biochem. Biophys. Res. Commun.* **2001**, *282*, 580−588.
(8) Giovannoni, M. P.; Dal Piaz, V.; Kwon, B. M.; Kim, M. K.; Kim Y. K.; Toma, L.; Barlocco, D.; Bernini, F.; Canavesi, M. 5,6-Diphenylpyridazine derivatives as acyl-CoA: cholesterol acyltransferase inhibitors. *J. Med. Chem.* **2001**, *44*, 4292−4295.
(9) Toma, L.; Nava, D.; Celentano, G.; Giovannoni, M. P.; Dal Piaz, V.; Kwon, B. M.; Kim, M. K.; Kim, Y. K.; Barlocco, D. 5,6-Dinitrophenyl and 5-aminophenyl-6-nitrophenyl analogues of the ACAT inhibitor 5,6-diphenyl-3-alkylaminopyridazines. *Heterocycles* **2000**, *53*, 2709−2718.
(10) Toma, L.; Giovannoni, M. P.; Dal Piaz, V.; Kwon, B. M.; Kim, Y. K.; Gelain, A.; Barlocco, D. Mono- and di-substituted 5,6-diphenyl-3-alkylamino-pyridazines active as ACAT inhibitors. *Heterocycles* **2002**, *57*, 39−46.
(11) Toma, L.; Giovannoni, M. P.; Vergelli, C.; Dal Piaz, V.; Kwon, B. M.; Kim, Y. K.; Gelain, A.; Barlocco, D. Novel 3-arylamino- and 3-cycloalkylamino-5,6-diphenyl-piridazines active as ACAT inhibitors. *Arch. Pharm. Pharm. Med. Chem.* **2002**, *11*, 563−566.
(12) Higley, C. A.; Wilde, R. G.; Maduskuie, T. P.; Johnson, A. L.; Pennev, P.; Billheime, J. T.; Robinson, C. S.; Gilles, P. J.; Wexler, R. R. Acyl CoA: cholesterol acyltransferase (ACAT) inhibitors: synthesis and structure−activity relationship studies of a new series of trisubstituted imidazoles. *J. Med. Chem.* **1994**, *37*, 3511−3522.
(13) Coates, W. J.; McKillop, A. One-pot preparation of 6-substituted 3(2*H*)-pyridazinones from ketones. *Synthesis* **1993**, *3*, 334−342.
(14) Wermuth, C. G.; Bourguignon, J. J.; Schlewer, G.; Gies, J. P.; Schoenfelder, A.; Melikian, A.; Bouchet, M. J.; Chantreux, D.; Molimard, J. C.; Heaulme, M. Synthesis and structure−activity relationships of a series of aminopyridazine derivatives of γ-aminobutyric acid acting as selective GABA-A antagonists. *J. Med. Chem.* **1987**, *30*, 239−249.
(15) Burnett, J. R.; Wilcox, L. J.; Huff, M. W. Acyl coenzyme A: cholesterol acyltransferase inhibition and hepatic apolipoprotein B secretion. *Clin. Chim. Acta* **1999**, *286*, 231−242.
(16) Jeong, T. S.; Kim, S. U.; Son, K. H.; Kwon, Y. K.; Choi, M. U.; Bok, S. H. GERI−BP001 compounds, new inhibitors of acyl-CoA: cholesterol acyltransferase from *Aspergillus fumigatus* F37 I. Production, isolation and physicochemical and biological properties. *J. Antibiot.* **1995**, *48*, 751−756.
(17) Cho, K. H.; An, S.; Lee, W. S.; Paik, Y. K.; Kim, Y. K.; Jeong, T. S. Mass-production of human ACAT-1 and ACAT-2 to screen isoform-specific inhibitor: a different substrate specificity and inhibitory regulation. *Biochem. Biophys. Res. Commun.* **2003**, *309*, 864−872.
(18) Brecher, P.; Chan, C. T. Properties of acyl-CoA: cholesterol O-acyltransferase in aortic microsomes from atherosclerotic rabbits. *Biochim. Biophys. Acta* **1980**, *617*, 458−471.
(19) Gaussian 03, Revision B.02, Frisch, M. J.; Trucks, G. W.; Schlegel, H. B.; Scuseria, G. E.; Robb, M. A.; Cheeseman, J. R.; Montgomery, J. A., Jr.; Vreven, T.; Kudin, K. N.; Burant, J. C.; Millam, J. M.; Iyengar, S. S.; Tomasi, J.; Barone, V.; Mennucci, B.; Cossi, M.; Scalmani, G.; Rega, N.; Petersson, G. A.; Nakatsuji, H.; Hada, M.; Ehara, M.; Toyota, K.; Fukuda, R.; Hasegawa, J.; Ishida, M.; Nakajima, T.; Honda, Y.; Kitao, O.; Nakai, H.; Klene, M.; Li, X.; Knox, J. E.; Hratchian, H. P.; Cross, J. B.; Adamo, C.; Jaramillo, J.; Gomperts, R.; Stratmann, R. E.; Yazyev, O.; Austin, A. J.; Cammi, R.; Pomelli, C.; Ochterski, J. W.; Ayala, P. Y.; Morokuma, K.; Voth, G. A.; Salvador, P.; Dannenberg, J. J.; Zakrzewski, V. G.; Dapprich, S.; Daniels, A. D.; Strain, M. C.; Farkas, O.; Malick, D. K.; Rabuck, A. D.; Raghavachari, K.; Foresman, J. B.; Ortiz, J. V.; Cui, Q.; Baboul, A. G.; Clifford, S.; Cioslowski, J.; Stefanov, B. B.; Liu, G.; Liashenko, A.; Piskorz, P.; Komaromi, I.; Martin, R. L.; Fox, D. J.; Keith, T.; Al-Laham, M. A.; Peng, C. Y.; Nanayakkara, A.; Challacombe, M.; Gill, P. M. W.; Johnson, B.; Chen, W.; Wong, M. W.; Gonzalez, C.; Pople, J. A., Gaussian, Inc., Pittsburgh, PA, 2003.

JM050703X